Key Engineering Materials Vol. 196 (2001) pp 53-60

doi:10.4028/www.scientific.net/KEM.196.53

Grinding of Ceramics: Strength, Surface Features and Grinding Conditions

Tianshun Liu[1], Bruno A. Latella[1] and Liangchi Zhang[2]

[1] Materials Division, ANSTO, Menai NSW 2234, Australia

[2] Dept. of Mechanical & Mechatronic Eng., The University of Sydney, Sydney NSW 2006, Australia

Keywords: Ceramics, Grinding, Grinding Conditions, Modulus of Rupture, Strength, Tetragonal to Monoclinic Transformation

ABSTRACT

The strength dependence of ceramics on microstructure, surface features and grinding conditions were studied in this work. A SiC and three 12Ce-TZPs with different grain sizes were ground under specific grinding conditions using two diamond-grinding machines. The normal grinding force increases with table speed, depth of cut and removal rate. Examination of the surface features show that the surface roughness in SiC and 12Ce-TZPs and the stress-induced t-m transformation in the 12Ce-TZPs strongly depend on the grinding conditions. The bending strength of the 12Ce-TZP with smaller grain size is not sensitive to the imposed grinding conditions. The strength of the 12Ce-TZP with the largest grain size and the SiC, however, is more sensitive to the grinding conditions. For the 12Ce-TZPs the grain size and the amount of the stress-induced t-m transformation dominate their strength.

1. INTRODUCTION

Advanced ceramics, such as silicon nitride, silicon carbide and zirconia (ZrO_2), are attractive in many engineering applications because of their high strength at elevated temperatures, corrosion resistance, high hardness and remarkable wear resistance. However, the use of ceramics has been limited mainly due to their brittle nature and high cost of machining. Machining induced damage can cause premature failure. Thus the relationship between the grinding conditions, the surface features generated, such as surface roughness and surface and sub-surface damage, microstructure and the strength of a ground ceramic component, has long been one of the central topics of research in the fields of machining and materials engineering [1-7]. The objective of this work was to study the effect of grinding conditions on subsurface damage, stress induced tetragonal to monoclinic (t-m) transformation in ZrO_2 and strength.

2. EXPERIMENTAL PROCEDURES

Four materials were studied: a commercial sintered SiC and three laboratory-produced 12mol% CeO_2 stabilised tetragonal zirconia polycrystal (12Ce-TZPs) of different grain size. The various grain sizes were obtained by sintering the 12Ce-TZP materials at different temperatures. Microstructure and subsurface damage caused by grinding were examined on polished and fracture surfaces, respectively, using scanning electron microscopy (SEM). Density was measured using the water displacement method. Young's modulus was measured using an impulse excitation technique (Grindo Sonic Mk5). Hardness was measured with a Vickers hardness tester at a load of 10kg. For

the 12Ce-TZP ceramics R-curves were measured from compact tension (CT) tests. Details of the CT tests have been described previously [8].

Diamond grinding was performed on two grinding machines: a numerically controlled grinding machine, the Junior CF CNC (Mini M286), and a manual grinding machine (Kent). Diamond-grinding wheels with 400 grit size were used. Grinding conditions are listed in Table 1. The removal rate was calculated from the table speed, depth of cut and specimen width. For grinding with the Mini M286 machine, the grinding force was monitored using a load cell located beneath the working table.

After grinding, the modulus of rupture (MOR) was measured in four-point bending using an Instron testing machine (Model 8562). The specimen sizes were 5×5×50mm and 5×4.5×38mm for the SiC and 12Ce-TZPs, respectively. The inner/outer span widths of the four-point bending tests were 20/40mm for the SiC and 17/34mm for the 12Ce-TZPs. These tests were conducted in position control with a loading rate of 1μm/s. Three to seven specimens were tested for each grinding condition.

Surface roughness was measured on all ground surfaces using a Profilometer (Alpha-Step 200). For the 12Ce-TZPs, the stress induced t-m phase transformation was measured on both ground and fracture surfaces using X-ray diffraction (XRD) (Siemens D500).

Table 1 Summary of the grinding conditions.

Material	Grinding machine	Table speed [mm/s]	Depth of cut [μm]	Removal rate [mm^3/s]
SiC	Mini M286	0.5	125	0.31
SiC	Mini M286	1.0	125	0.63
SiC	Mini M286	2.0	125	1.25
SiC	Kent	150	10	7.5
12Ce-TZPs	Mini M286	0.5	125	0.29
12Ce-TZPs	Mini M286	1.0	125	0.59
12Ce-TZPs	Mini M286	1.0	250	1.18
12Ce-TZPs	Mini M286	1.0	500	2.35
12Ce-TZPs	Mini M286	2.5	125	1.47
12Ce-TZPs	Kent	150	10	7.5

3. EXPERIMENTAL RESULTS

Table 2 gives the grain size, density, hardness, Young's modulus and fracture toughness of the four materials. Due to the stress induced t-m transformation, the three 12Ce-TZPs exhibit pronounced R-curve behaviour. The crack resistance increases from K_{Ii} to K_{Imax} over a crack extension of about 1mm. Both K_{Ii} and K_{Imax} of 12Ce-TZP-I are less than those of 12Ce-TZP-II and -III. The fracture toughness of the SiC is much lower than the three 12Ce-TZPs.

Table 2 Characterisation of the four materials tested.

Materials	Grain size [μm]	Density [kg/cm^3]	Vicker's Hardness [kg/mm^2]	Young's Modulus [GPa]	K_{Ii} [$MPa*m^{0.5}$]	K_{Imax} [$MPa*m^{0.5}$]
12Ce-TZP-I	1.8	6.22	748	202	5.3	6.3
12Ce-TZP-II	4.1	6.23	810	200	6.3	6.9
12Ce-TZP-III	7.2	6.22	801	197	6.2	7.0
SiC	4.0	3.20	--	455	--	5.2

Figure 1 shows the MOR of the four materials as a function of table speed at a constant depth of cut of 125μm. The MOR of 12Ce-TZP-I and -II with smaller grain sizes are not sensitive to the table speed. The 12Ce-TZP-III and SiC, however, exhibit a peak MOR at a table speed of 1mm/s. For the 12Ce-TZPs the MOR increases with larger grain size at all grinding conditions. The SiC exhibits lower MOR than the 12Ce-TZPs. Figure 2 shows the MOR as a function of depth of cut at a constant table speed of 1mm/s. For 12Ce-TZP-I, the MOR is not sensitive to the depth of cut. For 12Ce-TZP-II and -III, however, the MOR is higher at the smallest depth of cut of 125μm.

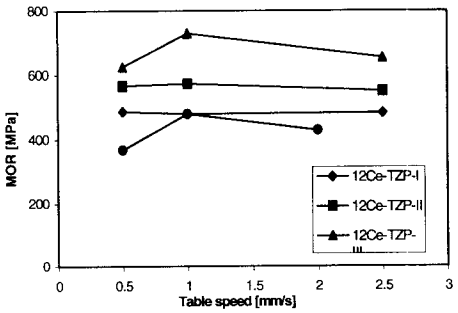

Fig. 1 MOR as a function of table speed at a constant depth of cut of 125μm.

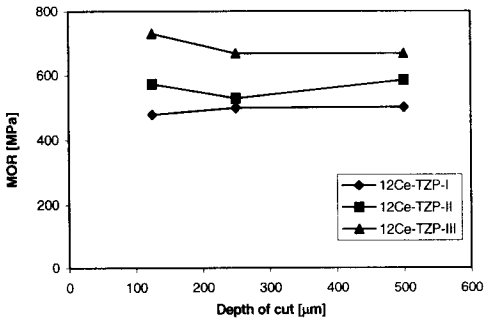

Fig. 2 MOR as a function of depth of cut at a constant table speed of 1mm/s.

Figure 3 shows MOR as a function of removal rate. Since the removal rate depends on the table speed and depth of cut, the MOR dependence on removal rate is influenced by both grinding parameters. The highest removal rate represents a table speed of 150mm/s and depth of cut of 10μm. This grinding condition resulted in the highest MOR for all three 12Ce-TZPs but the lowest MOR for the SiC. There is no clear correlation between the removal rate and the MOR.

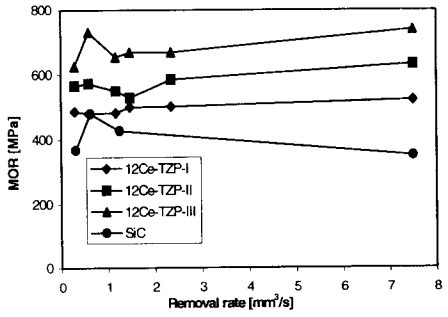

Fig. 3 MOR as a function of removal rate.

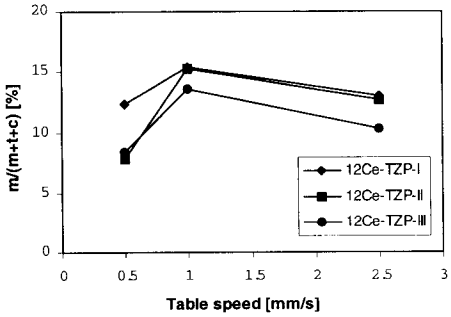

Fig. 4 Amount of ground surface stress induced t-m phase transformation as a function of the table speed.

Figures 4, 5 and 6 show the amount of stress induced tetragonal to monoclinic (t-m) phase transformation of the 12Ce-TZPs on the ground surface as a function of the table speed, depth of cut and removal rate, respectively. The amount of the t-m transformation is slightly lower for 12Ce-TZP-III with the largest grain size. The peak amount of t-m transformation occurs at a table speed of 1mm/s, as shown in Figure 4. The degree of the stress-induced t-m transformation does not depend on the depth of cut, except at a depth of cut of 250 μm where 12Ce-TZP-III shows less transformation. There is no clear correlation between the amount of t-m transformation and the removal rate.

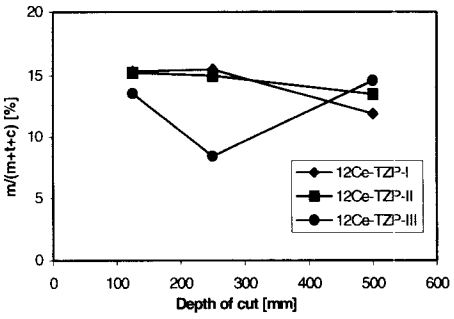

Fig. 5 Amount of ground surface stress induced t-m phase transformation as a function of the depth of cut.

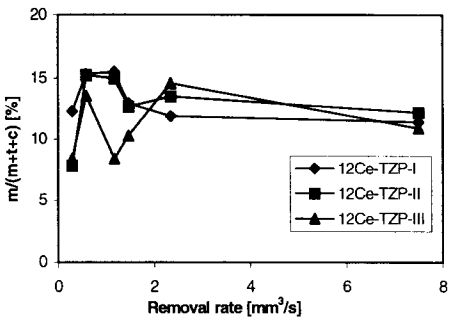

Fig. 6 Amount of ground surface stress induced t-m phase transformation as a function of the removal rate.

Figures 7 and 8 show the amount of stress induced t-m transformation on the fracture surfaces under different grinding conditions. As expected, the stress-induced transformation on the fracture surface does not vary with the grinding conditions. The 12Ce-TZP-III with the largest grain size exhibits less transformation than 12Ce-TZP-I and -II.

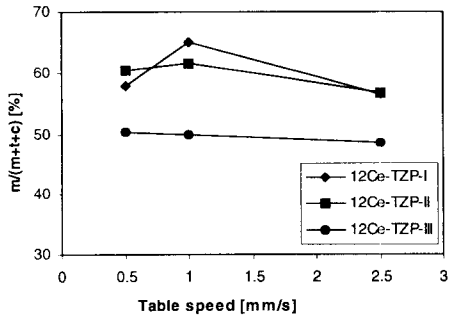

Fig. 7 Effect of table speed on stress induced t-m transformation on the fracture surface.

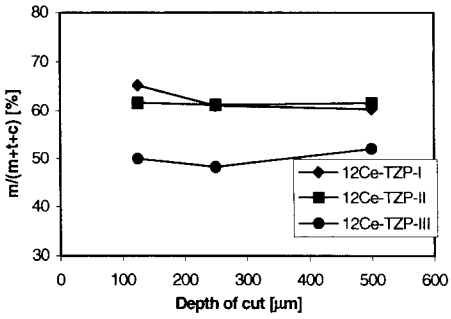

Fig. 8 Effect of depth of cut on stress induced t-m transformation on the fracture surface.

Figures 9, 10 and 11 show the normal grinding force as a function of table speed, depth of cut and removal rate, respectively. The grinding force increases with increasing table speed, depth of

cut and removal rate. There is no significant difference in the grinding force between the three 12Ce-TZPs. However, the grinding force of the SiC is slightly lower than that of the 12Ce-TZPs.

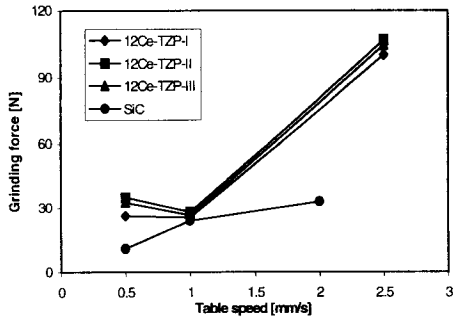

Fig. 9 Effect of table speed on normal grinding force.

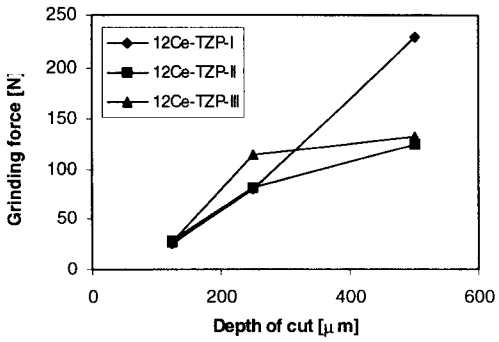

Fig. 10 Effect of depth of cut on normal grinding force.

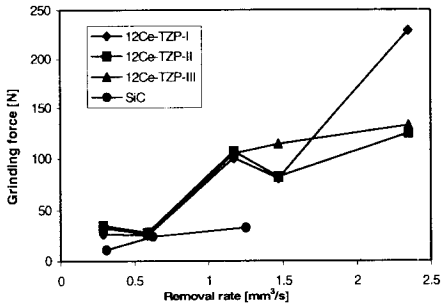

Fig. 11 Effect of material removal rate on normal grinding force.

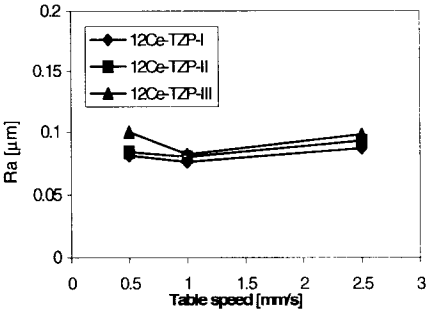

Fig. 12 Effect of table speed on average roughness, R_a.

Figures 12, 13 and 14 show the average surface roughness, R_a, as a function of the table speed, depth of cut and removal rate, respectively. The R_a does not vary significantly with the table speed and depth of cut. However, the highest removal rate (Figure 14), where table speed and depth of cut are 150mm/s and 10μm, respectively, yielded the highest R_a. The maximum roughness, R_{max}, was also measured using the roughness tester. The measured R_{max} is about one order of magnitude higher than the average roughness, R_a. There is no apparent correlation between R_{max} and the grinding conditions.

Figure 15 shows the Weibull plot of the MOR, where specimens from all grinding conditions were included in the calculation of the failure probability, *F*. The Weibull modulus is 32, 17, 12 and 6 for the 12Ce-TZP-I, -II, -III and SiC respectively. The 12Ce-TZP-I with the smallest grain size exhibits the highest Weibull modulus of 32. The 12Ce-TZP-II and -III with increased grain size exhibit much lower Weibull modulus of 17 and 12, respectively. The SiC shows the lowest Weibull modulus of 6, which is much lower than the value of 18 given by the manufacturer.

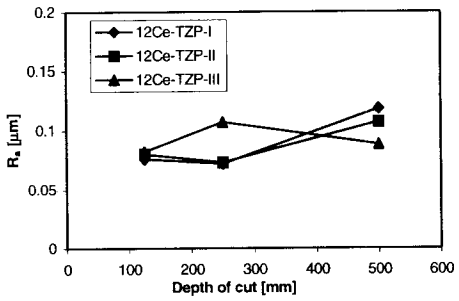

Fig. 13 Average roughness as a function of the depth of cut.

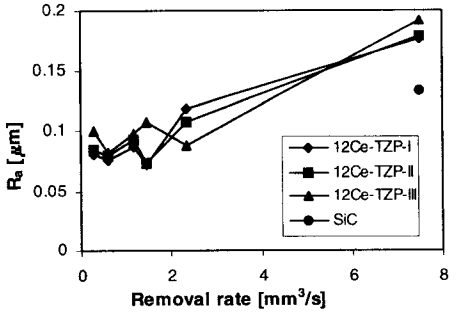

Fig. 14 Average roughness as a function of the removal rate.

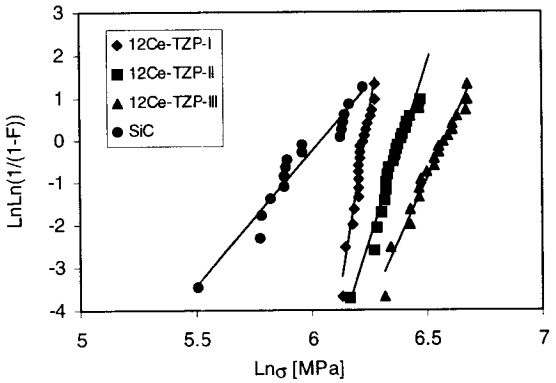

Fig. 15 Weibull plot of the MOR of the four materials.

4. DISCUSSION

In general, the MOR of a ceramic material depends on intrinsic and extrinsic factors. The intrinsic factors include fracture toughness and processing flaw distribution. The extrinsic factors include extent of the surface and sub-surface damage due to grinding, residual stress state, surface roughness, and, in the case of 12Ce-TZP ceramics, the grinding induced t-m transformation on the ground surface. While the intrinsic factors do not depend on the grinding conditions, the extrinsic factors are strongly related to them.

With respect to the intrinsic factors, the MOR can be represented as a function of the fracture toughness, K_{Ic}, and the critical flaw size, a_c, given by the following equation:

$$K_{Ic} = 2\sigma\sqrt{\frac{a_c}{\pi}} \qquad (1)$$

where σ is the MOR. The higher toughness of the 12Ce-TZPs compared to the SiC is caused by the stress-induced t-m transformation toughening, which is well known in zirconia based ceramics [9]. For the 12Ce-TZPs it is not clear why the 12Ce-TZP-III with the largest grain size has the lowest amount of stress induced t-m transformation (see Figures 4-8) and the highest fracture toughness, K_{Ic}. SEM examination of the fracture surfaces reveal that 12Ce-TZP-I showed intergranular fracture, while the 12Ce-TZP-II and -III displayed a much higher proportion of transgranular fracture, as shown in Figure 16. Nevertheless the higher fracture toughness of 12Ce-TZP-II and -III has contributed to a higher MOR for these two materials for all grinding conditions.

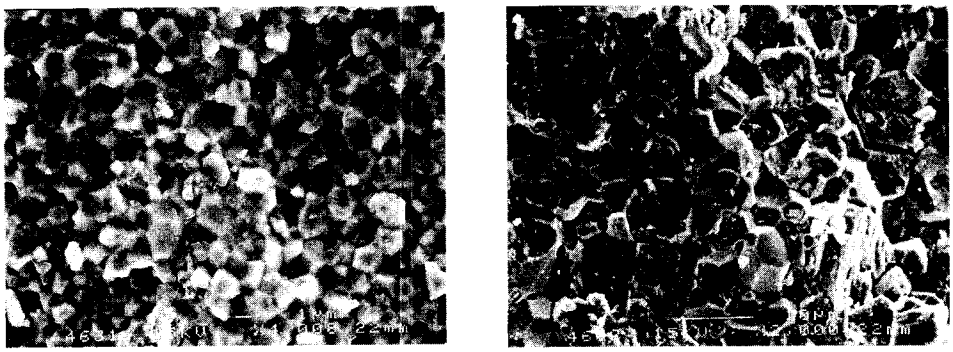

(a) 12Ce-TZP-I (b) 12Ce-TZP-III

Fig. 16 SEM images of the fractured surfaces.

With respect to the extrinsic factors, two grinding parameters were varied, that is, the table speed and depth of cut. Due to these two changes the removal rate and grinding force also varied. The grinding force is an important indirect grinding parameter. It provides an indication of contact stresses acting on the specimen surface. The extent of grinding damage will strongly depend on the grinding force. For the materials studied in this work, the grinding force increased with increasing table speed, depth of cut and removal rate. The grinding forces were higher for the 12Ce-TZPs compared with the SiC. Further work is required to characterise the surface and sub-surface damage after grinding as well as its dependence on the grinding force.

From the measured R-curves and MOR, the critical flaw sizes were estimated using equation 1. The range of flaw sizes is 78-116, 68-151, 49-112 and 83-348μm for the 12Ce-TZP-I, -II, -II and SiC, respectively. It is not clear whether these flaws were more processing related or micro-cracking damage caused by grinding. The MOR data shown in Figures 1, 2, 3 and 15, however, do indicate that 12Ce-TZP-I with the smallest grain size is less sensitive to the grinding conditions, resulting in the highest Weibull modulus for this material. With increased grain size 12Ce-TZP-II and -III are more sensitive to the grinding conditions. Therefore, the Weibull modulus is much lower for 12Ce-TZP-II and -III. The SiC is more sensitive to the grinding conditions than the 12Ce-TZPs despite its relatively small grain size. This is probably due to the fact that there is no stress-induced transformation on the as-ground surface. The stress induced t-m transformation in the 12Ce-TZPs can introduce a compressive stress field in the surface and sub-surface region, which can reduce the grinding sensitivity in the 12Ce-TZPs.

The surface roughness, R_a and R_{max}, do not seem to be dependent on the grinding conditions, except at much higher table speed (150mm/s) and smaller depth of cut (10μm). Since the R_a and R_{max} are nearly three and two orders of magnitude lower than the estimated critical flaw sizes, the

MOR of the four materials studied in this work is not controlled by the surface roughness under the given grinding conditions.

Since the MOR depends on many factors, correlations between the MOR and grinding conditions is complex. Two important extrinsic factors, that is, the residual stress and surface and sub-surface damage, need to be explored further to understand the interrelationships between the grinding conditions and the MOR.

5. CONCLUSIONS

The effect of grinding on surface integrity and MOR of a SiC and three 12Ce-TPZs ceramics were studied. The results are summarised as follows:

(a) The MOR of the 12Ce-TZPs increased with larger grain size for all grinding conditions. This is partially caused by higher K_{Ic} with larger grain size. The 12Ce-TZP-III with the largest grain size seemed to be more sensitive to the imposed grinding conditions.

(b) The MOR of the SiC was much lower than the 12Ce-TZPs at all grinding conditions. Likewise, the MOR of the SiC was found to be more sensitive to the grinding conditions than the 12Ce-TZPs despite its relatively small grain size.

(c) The grinding force increased with increased depth of cut, table speed and removal rate for all materials studied. The grinding force was higher for the 12Ce-TZPs than for the SiC.

(d) The average surface roughness was measured to be nearly three orders of magnitude smaller than the estimated "critical flaw size", indicating that it does not control the strength of the materials.

ACKNOWLEDGMENT

Liangchi Zhang thanks the Australian Research Council for its financial support to the present research.

REFERENCES

[1] L Zhang, Grindability of some metallic and ceramic materials in CFG regimes, *Int. J. Mach. Tools Manfact.*, **34**(8) (1994) 1045-1057.

[2] I Zarudi, L Zhang and Y W Mai, Subsurface damage in alumina induced by single point scratching, *J. Mat. Sci.*, **31** (1996) 905-914.

[3] S Malkin, Grinding mechanisms for ceramics, *Ann. CIRP*, **45**(2) (1996) 569-580.

[4] R Komanduri, D A Lucas and Y Tani, Technological advances in fine abrasive processes, *Ann. CIRP*, **46**(2) (1997) 545-596.

[5] I Zarudi, L Zhang and D Cockayne, Subsurface structure of alumina associated with single-point scratching, *J. Mat. Sci.*, **33** (1998) 1639-1654.

[6] I Zarudi and L Zhang, Initiation of dislocation systems in alumina in single-point grinding, *J. Mat. Res.*, **14** (1999) 1430-1436.

[7] I Zarudi and L Zhang, On the Limit of Surface Integrity of Alumina by Ductile-Mode Grinding, *Trans ASME, J. Engg Mat. Tech.*, **122** (2000) 129-134.

[8] T S Liu, Y W Mai, M V Swain and G Grathwohl, Effects of grain size and specimen geometry on the transformation and R-curve behaviours of 9Ce-TZP ceramics, *J. Mat. Sci.*, **29** (1994) 835-843.

[9] R G Garvie, R H J Hannink and R T Pascoe, Ceramic steel, *Nature*, **258** (1975) 703-704.

Precision Machining of Advanced Materials
doi:10.4028/www.scientific.net/KEM.196

Grinding of Ceramics: Strength, Surface Features and Grinding Conditions
doi:10.4028/www.scientific.net/KEM.196.53